INSTITUTE OF PHYSICS PUBLISHING JOURNAL OF PHYSICS: CONDENSED MATTER

J. Phys.: Condens. Matter **17** (2005) 7689–7704 doi:10.1088/0953-8984/17/48/019

Spectral momentum densities of vanadium and vanadium oxide as measured by high energy (e, 2e) spectroscopy

C Chen, M N Gale, A S Kheifets, M Vos[1] and M R Went

Atomic and Molecular Physics Laboratories, Research School of Physical Sciences and Engineering, Australian National University, Canberra ACT 0200, Australia

E-mail: maarten.vos@anu.edu.au

Received 4 January 2005, in final form 12 October 2005
Published 11 November 2005
Online at stacks.iop.org/JPhysCM/17/7689

Abstract

The spectral momentum densities of vanadium metal and V_2O_3 are measured by electron momentum spectroscopy. Results are compared with band structure calculations based on density functional theory (DFT). Qualitatively, the agreement between theory and experiment is good. The calculated total band width of vanadium metal (6.5 eV) is in excellent agreement with the observed one (6.5 $\pm$ 0.25 eV). The splitting between the outer and inner valence bands in V_2O_3 is 2 eV larger in the experiment than in the density functional theory calculation. The observed momentum distributions agree reasonably well with the calculated distributions with the exception of the intensity of the outer valence band relative to the inner valence band in V_2O_3: the outer valence band is less intense than calculated. The momentum density near the Fermi level in V metal resembles that of atomic V 3d orbitals. However, momentum profiles of the V 3d orbitals in V_2O_3 are much more sharply peaked than the atomic 3d orbital in both the theory and experiment. Correlation effects are discussed and theoretical problems in describing EMS data from narrow band systems are identified.

(Some figures in this article are in colour only in the electronic version)

1. Introduction

Electron momentum spectroscopy (EMS) has shown in recent years that it can measure spectral momentum densities of matter directly [1]. It has a completely different foundation compared to angular resolved photo-emission, the standard technique for the determination of band structure. EMS is a collision experiment and the measured intensity is directly proportional

[1] Author to whom any correspondence should be addressed.

to the spectral function of the target. Within a one-particle picture the measured intensity is simply proportional to the probability that a target electron has a certain combination of binding energy and momentum.

In the last few years, the technique has been tested for several 'simple' cases, where the samples are considered to be well understood materials. For example, single crystals of graphite [2], silicon [3, 4] and copper [5] were studied. In general, it became clear that, in spite of multiple scattering, quantitative information can be obtained by EMS, and even for the simple cases reasonable agreement between measurement and theory can be obtained only if many-body effects are incorporated in the theory.

Now, as the validity of the technique is well established, we want to start focusing on more complicated cases, where band structure calculations fail to predict even the most basic properties of materials. One such example is V_2O_3, a material that has a phase transition from a antiferromagnetic insulating phase to an paramagnetic metallic phase at $\approx$150 K and a second transition at $\approx$500 K from the paramagnetic metallic phase to a paramagnetic insulating phase. This paper describes the first step of this project, a comparison of the EMS spectra of vanadium metal and the metallic V_2O_3 phase to those calculated using density functional theory.

In spite of the somewhat basic sample preparation procedures (polycrystalline thin vanadium and V_2O_3 films supported on a thin carbon film, as well as single-crystalline V_2O_3 films), the technique reveals interesting insights into the electronic structure of these materials. There has been very little theory developed for EMS of narrow band systems. As we show here that these measurements are becoming possible we want to stress the need for such a theory. Several possible experiments that might provide new tests for theories are discussed.

2. Experimental technique

In the high-energy high-resolution EMS spectrometer, which is fully described elsewhere [6], a well collimated beam of 50 keV electrons is incident on a thin self-supporting sample. The incident and ejected electrons emerge with nearly equal energies (25 keV) and polar angles ($\sim$45°) relative to the incident (z) direction. The use of such high energies for the incident and emitted electrons greatly reduces the multiple scattering effects, which plagued earlier measurements [7]. The energies and azimuthal angles of the emitted electrons, detected in coincidence, are measured with electrostatic analysers fitted with two-dimensional position-sensitive detectors [6]. In high-energy EMS the incoming and outgoing electrons can be accurately treated as plane waves. Knowing their energies E_i and momenta $\boldsymbol{k}_i$ one can infer the binding energy ω and momentum $\boldsymbol{q}$ of the struck electron before the collision through the conservation laws

$$\omega = E_0 - E_1 - E_2, \qquad \boldsymbol{q} = \boldsymbol{k}_1 + \boldsymbol{k}_2 - \boldsymbol{k}_0, \tag{1}$$

where the subscripts $i = 0, 1, 2$ refer to the incident and emitted (scattered and ejected) electrons, respectively.

If the mean scattering plane (horizontal) is defined as the x–z plane, then the momentum component q_y is determined by the relative azimuthal angles ϕ_1, ϕ_2 of the two detected electrons. The momentum components in the x- and z-directions are determined by the choice of polar angles θ_1 and θ_2. In the present case the polar angles were both fixed at 44.3° so that $q_x = q_z = 0$. Different choices of θ_1 and θ_2 about 44.3° give other values for q_x and q_z, in which case the measurements are along lines in momentum space that do not go through $q = 0$ (a Γ point) [6].

In EMS, the measurement involves real momenta and it does not depend on the crystal lattice. This applies to (gas-phase) atoms and molecules and amorphous materials as well

as it does to the present case of single-crystalline and polycrystalline materials. For the polycrystalline samples we can measure the spherically averaged spectral function. The spherically averaged spectra will generally be broader and show less structure than those obtained for a single crystal. However, the spectrum at zero momentum is not affected by the averaging procedure. The energy and momentum resolution are 1.0 eV and 0.1 au respectively (1 au of momentum corresponds to 1.89 $Å^{-1}$; 1 au of length equals 0.529 Å).

EMS is a transmission spectroscopy that requires extremely thin free-standing films. Vanadium metal films were evaporated on a thin (30 Å thick) free-standing amorphous carbon film. The thickness of the vanadium layer was approximately 100 Å, as judged from a crystal thickness monitor. Some of the (e, 2e) events will occur in the carbon layer. This will cause a signature of the carbon spectral function in the data. However, in this case two electrons have to traverse the vanadium layer with a relatively high probability of elastic and inelastic scattering. Thus, the contribution of the carbon layer is less than that expected just from the ratio of the thicknesses. The signature of the carbon layer can be subtracted, in first approximation, using the measured spectral function of a carbon film.

V_2O_3 films were obtained by evaporating V in a oxygen atmosphere (10^{-6} Torr). This is known to produce samples with a stoichiometry of V_2O_3 (see e.g. [8]). Some films were annealed in 10^{-6} Torr of oxygen after deposition. No clear influence of annealing on the measured EMS data was observed, indicating that the measured electronic structure is not very sensitive to the degree of long-range order. However, only those samples annealed above $\simeq$300 °C showed distinct diffraction rings.

It turned out that it was rather straightforward to grow single-crystal V_2O_3 films. V_2O_3 grows epitaxially on the Au ⟨111⟩ surface [8]. A thin epitaxial Au film ($\approx$1000 Å thick) was grown epitaxially on NaCl with a ⟨111⟩ surface normal. The NaCl was dissolved and the Au film was transferred to the sample holder. V_2O_3 films were grown on the free-standing Au film by evaporating in an oxygen atmosphere and annealed to a few hundred °C. The Au film was subsequently removed by sputtering.

3. Theory

The energy bands and corresponding momentum densities were calculated using the full-potential linear muffin-tin orbital (FP-LMTO) method calculation as described in [9].

3.1. Vanadium

Vanadium metal was calculated in the BCC structure (space group 229 $Im\bar{3}m$) with the lattice parameter $a = 5.71$ au. The muffin-tin radius was chosen to be one half of the nearest neighbour distance $d_{V-V} = \sqrt{3}/2a$, $R = 0.5d_{V-V} = 2.47$ au.

Energy bands $E_j(\boldsymbol{q})$ and momentum densities $\rho_j(\boldsymbol{q})$ as functions of the momentum in several high-symmetry directions in vanadium are shown in figure 1. From these quantities, the energy resolved (or spectral) momentum density was calculated as

$$A(\boldsymbol{q}, \omega) = \sum_j \sum_{\boldsymbol{G}\boldsymbol{k}} \rho_j(\boldsymbol{q}) \delta_{\boldsymbol{q},\boldsymbol{k}+\boldsymbol{G}} \delta(\omega - E_j(\boldsymbol{k})). \tag{2}$$

Here $\boldsymbol{q}$ and $\boldsymbol{k}$ are the real and crystalline momenta, respectively, connected by a reciprocal lattice vector $\boldsymbol{G}$. The spectral momentum density was then averaged over 64 directions sampling the irreducible wedge of the BCC Brillouin zone. The spherical averaging was required due to the fact that we have polycrystalline samples. To make a comparison with the experiment, the spectral momentum density (equation (2)) was convoluted with a Gaussian to simulate

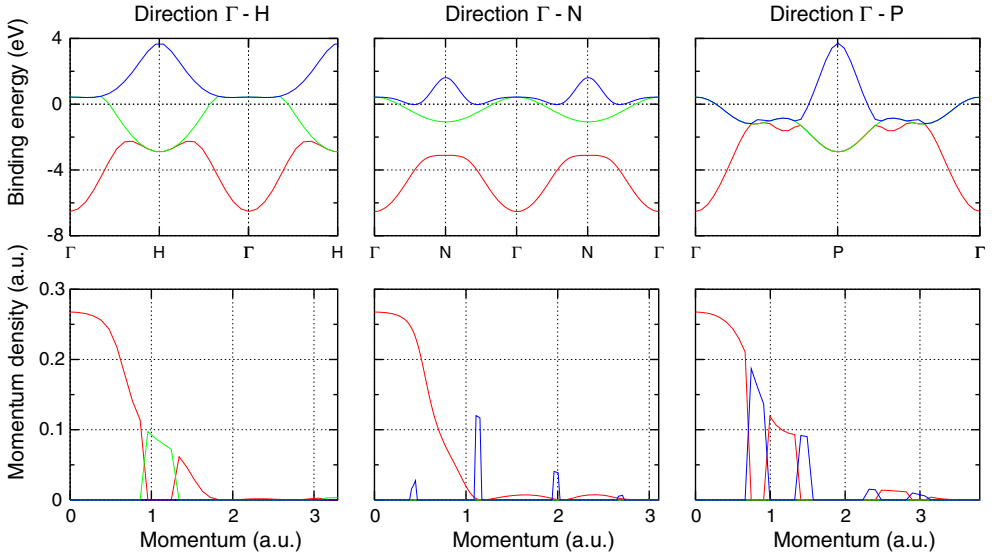

Figure 1. Energy bands (top row) and momentum densities (bottom row) in various high-symmetry directions of BCC vanadium. Corresponding bands are indicated by same line stiles in both rows of plots. The dispersion and momentum densities are plotted over the same momentum range, but in the dispersion plot the axes are labelled by the symmetry points.

an energy resolution of 1 eV. For the V metal case, we also did calculations incorporating a semi-empirical lifetime broadening, with the Lorentzian broadening dependent on the binding energy as follows from the electron gas theory [10].

3.2. Vanadium oxide

The vanadium oxide V_2O_3 was calculated in the corundum structure (space group 167 $R\bar{3}ch$). The Bravais lattice of corundum is trigonal with all the primitive lattice vectors of equal length $a = 10.66$ au forming an equal angle $\alpha = 53°45'$ between any two of them [11]. In Cartesian coordinates, the primitive lattice vectors are conveniently expressed in terms of the two constants, s and r [12]

$$\begin{pmatrix} \mathbf{t}_1 \\ \mathbf{t}_2 \\ \mathbf{t}_3 \end{pmatrix} = \begin{pmatrix} s \cdot \mathbf{e}_x & 0 \cdot \mathbf{e}_y & r \cdot \mathbf{e}_z \\ -s/2 \cdot \mathbf{e}_x & s\sqrt{3}/2 \cdot \mathbf{e}_y & r \cdot \mathbf{e}_z \\ -s/2 \cdot \mathbf{e}_x & -s\sqrt{3}/2 \cdot \mathbf{e}_y & r \cdot \mathbf{e}_z \end{pmatrix}, \tag{3}$$

where $s = 2a/\sqrt{3}\sin(\alpha/2) = 5.54$ au and $r = (a^2 - s^2)^{1/2} = 9.11$ au. In vanadium oxide, $r/a = 0.854$ and $s/a = 0.519$. The four vanadium positions are at

$$\pm[(1/4 \pm u)\boldsymbol{t}_1 + (1/4 \pm u)\boldsymbol{t}_2 + (1/4 \pm u)\boldsymbol{t}_3].$$

The six oxygen positions are at

$$\pm[(1/4 - v)\boldsymbol{t}_1 + (1/4 + v)\boldsymbol{t}_2 + 1/4\,\boldsymbol{t}_3]$$
$$\pm[(1/4 + v)\boldsymbol{t}_1 + 1/4\,\boldsymbol{t}_2 + (1/4 - v)\boldsymbol{t}_3]$$
$$\pm[1/4\,\boldsymbol{t}_1 + (1/4 - v)\boldsymbol{t}_2 + (1/4 + v)\boldsymbol{t}_3]$$

where $u = 0.096$ and $v = 0.315$. The muffin-tin radius was chosen to be one-half of the distance between the neighbouring vanadium and oxygen atoms $D_{\mathrm{V-Ox}} = 0.375a = 4.00$ au, $R = 0.5D_{\mathrm{V-Ox}} = 2.00$ au.

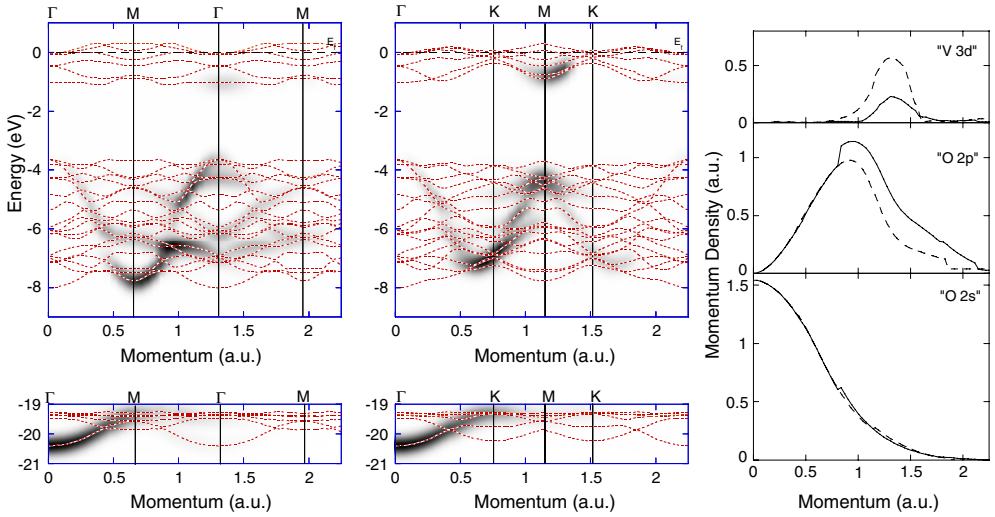

Figure 2. Energy bands along the Γ–M (left panel)and Γ–K (central panel) directions. The dispersion curves are superimposed on a grey-scale plot with an intensity proportional to the *calculated* spectral momentum density at each momentum–energy combination along a line from zero momentum to the closest M point (left panel) and along the line from zero momentum to the closest K point. The O 2s derived band is displayed in the lower half, the O 2p V 3d bands in the top half. The grey-scale intensity distribution is independently normalized in the top and lower halves. In the right panel we show the total density of the O 2s bands, O 2p bands and V 3d bands as a function of momentum for both directions for both the Γ–M direction (full line) and the Γ–K direction (dashed line).

Present calculated band energies were found to be in good agreement with the earlier DFT calculation [13]. The calculated band energies and momentum densities in one of the high-symmetry directions Γ–K and Γ–M are presented in figure 2. The whole band structure of V_2O_3 can be conveniently split into three sub-bands originating from the oxygen 2s (lower VB), the oxygen 2p (middle VB) and the vanadium 3d (upper VB) orbitals. Due to the orbital character, the momentum density in the lower VB peaks at zero momentum, whereas the density is zero at zero momentum for the middle and upper VB and their maximum densities are displaced towards larger momenta.

For single crystals we can align the measurement direction with a major crystallographic direction. In this case we can measure along a line through zero momentum to, for example, the closest K or M point. Fortunately the measured electronic structure simplifies under these conditions, as many bands do not contribute to the measurement. The amount a band contributes is proportional to the shading displayed in figure 2. To a first approximation the predicted pattern is rather similar for both directions. Indeed, even in the fully spherically averaged calculation these patterns survive. For example, for the O 2p derived band dispersion to higher binding energy, an increasing intensity up to 0.6 au followed by dispersion to lower binding energy and slow decrease in intensity is obtained in the calculation for the Γ–M direction and Γ–K direction as well as the spherically averaged case.

It is instructive to compare in figure 2 the theory for the M point reached at ≈0.6 au along the Γ–M direction and another M point at ≈1.1 au along the Γ–K direction. As these are equivalent points in the reduced zone scheme, the band energies are identical at both M points, but which band contributes to the measured intensity is completely different. For the 2p feature of the spectra we have maximum binding energy for the first M point, but approximately minimal binding energy for the second case.

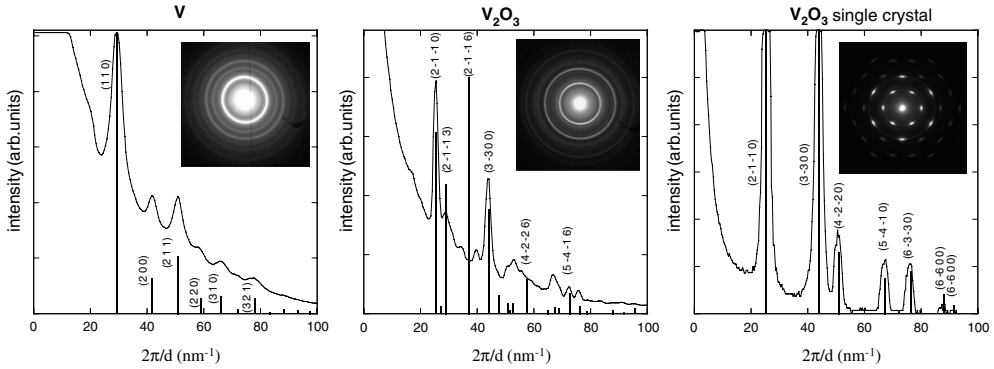

Figure 3. The radial intensity distribution of the diffraction patterns (shown as an inset) of vanadium and V_2O_3 films. The calculated intensity of the diffracted peaks are for a polycrystalline sample averaged over all orientations. The calculation fits the V metal distribution quite well, but completely fails to describe the V_2O_3 intensity distribution, indicating a preferential orientation in these films. For the single-crystal case we plot the maximum intensity at a certain radius, rather than the average intensity. Now only diffraction peaks due to reciprocal lattice vectors perpendicular to ⟨0001⟩ are observed.

The spectral momentum density (equation (2)) was generated from the data plotted in figure 2. Subsequently, energy broadening, to allow for the experimental energy resolution (and for polycrystalline sample spherical averaging), was applied before making comparison with the experiment.

Very small anisotropy was calculated for the momentum density of the O 2s derived band, that basically retains its atomic character. Slightly larger anisotropies were found for the 2p derived level. The V 3d band displayed very large anisotropies, as expected for a band that is only partly occupied.

4. Experimental results

Before each measurement a diffraction pattern was measured *in situ* in the spectrometer, and the results were compared with the calculated diffracted peak position as described by Lábár [14]. The results are shown in figure 3. For vanadium metal the observed rings had an intensity distribution that corresponds to the one calculated for a polycrystalline film. For the V_2O_3 film grown on carbon the observed intensity distribution is completely different from the calculated one. Diffraction peaks corresponding to reciprocal lattice vectors with a large component along the (0001) direction (the z-axis) are missing. This would correspond to V_2O_3 with the (0001) planes of the corundum structure close to parallel to the carbon film. Indeed, this growth mode is well known for V_2O_3 films on almost any surface [15]. Finally, for the V_2O_3 films grown on Au⟨111⟩ we get the diffraction pattern for a single crystal. For very thin V_2O_3 single-crystal film, suitable for EMS, the diffraction spots become somewhat elongated.

In figure 4 we show the spectral function of the vanadium metal film and the V_2O_3 film as measured by EMS. A faint contribution of the carbon spectrum was subtracted. The data are compared with the results of the full-potential linear muffin-tin orbital (FP-LMTO) calculation [9]. The calculation was convoluted with an experimental energy resolution of 1 eV. The same main features are evident in the experiment and theory, but the experimental distribution is broader (due to lifetime broadening and finite momentum resolution) and the contrast is lower (due to multiple scattering, i.e. elastic or inelastic scattering by one or more of

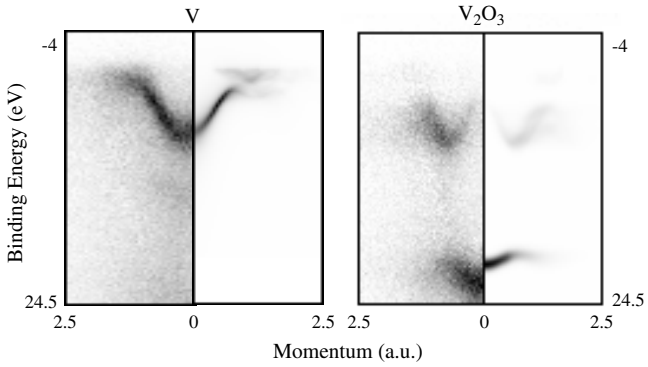

Figure 4. Measured (left half) and calculated (right half) spectral momentum densities of a vanadium film and a V_2O_3 film grown on carbon.

the high energy electrons). The vanadium metal results show a free-electron parabola, evolving in a broader, less intense distribution near the Fermi level. The free-electron part is due to the 4s electrons whereas the broader distribution near the Fermi level has mainly a 3d character.

EMS results of samples obtained by evaporation in an oxygen ambient show a completely different intensity distribution. Here the two main components are mainly derived from the O 2p levels (near 8 eV) and the O 2s levels (near 22 eV). There is a weak signal, hardly visible in these grey-scale plots, just below the Fermi level, originating from V 3d electrons. Within the O 2p related intensity, and to a minor extent in the O 2s related intensity, there is clear change in binding energy with momentum (dispersion). At zero momentum the 2s level has maximum binding energy and intensity, whereas the 2p level intensity approaches zero here, and has a minimum in binding energy. This behaviour is typical for the O 2s and O 2p derived orbitals in oxides [16]. In the grey-scale plot we have shown only the valence band region. However, the experimental data also contain the outer core levels of vanadium (3p and 3s). These core levels are more diffuse in momentum space, and hence a weaker signal is obtained. Reasonable statistics can be obtained by integrating the data over a 0.5 or 1.0 au wide momentum range. This is done in figure 5.

It is often somewhat problematic to pinpoint the exact Fermi level position in these measurements, as the shapes of the spectra are determined by both energy and momentum resolution [17]. In the V metal spectra, the V 3p level stands out as a relatively sharp feature and this is the easiest way to fix the energy scale. Recent XPS studies of vanadium metal give a binding energy of 37.2 eV for the V 3p level [18]. We aligned our energy scale so the V 3p core level coincides with this value. In contrast to XPS (x-ray photoelectron spectroscopy) we resolve the momentum of the core level. Thus, in theory, dispersion of the V 3p level could be measured. In contrast to the O 2s level there is no sign of dispersion in the V 3p binding energy. This sets an upper limit to the dispersion in the V 3p level of 0.25 eV.

The inset of figure 5 shows the spectra near zero momentum for the 100 Å thick V metal film together with that obtained for a much thinner film. For the thin film we can distinguish clearly three peaks; the peak at large binding energy resembles the spectra of carbon near zero momentum, both in position and shape [19]. The low binding energy peak lines up with the vanadium peak of the thick sample. We assign the middle peak to the bottom of the valence band of a carbon–vanadium compound formed at the interface. Its sharpness indicates that the interface layer contains a well defined phase. Contributions of both the carbon peak and the interface compound peak can be distinguished in the thick vanadium sample as well, but are much weaker. Using a measured spectral momentum density of a carbon foil we can

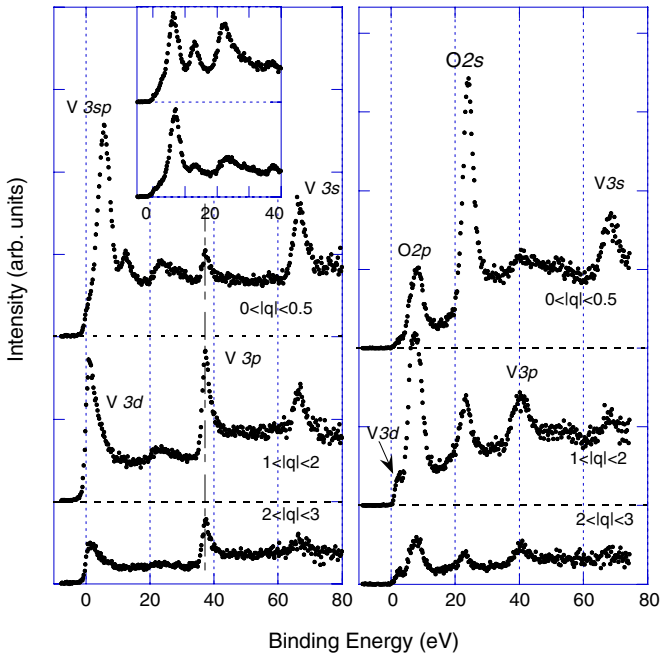

Figure 5. A comparison of the spectra for vanadium metal (left panel) and V_2O_3 (right panel) integrated over momentum intervals as indicated. The inset in the left panel shows spectra near zero momentum for the 100 Å thick vanadium sample (bottom) and a thinner vanadium sample (top), both supported by a 30 Å thick carbon film.

eliminate the small carbon contribution to the measured intensity of the 100 Å thick V sample by subtracting the appropriately scaled carbon intensity distribution. This was done for the results displayed in figure 4.

For the oxide spectra, the V 3p and 3s core levels are much broader compared to those in the V metal phase, a fact that is well known from XPS data [20]. It is therefore not convenient to fix the energy scale using this core level position. We put the Fermi level near the leading edge of the V 3d feature. The broad V 3p feature of the oxide is then several volts higher in binding energy than that of the metal, in agreement with the XPS data.

The large width of the core levels in V_2O_3 is often attributed to interaction between the core hole and the V 3d electrons, ligand holes in their narrow bands. A number of different discrete final states can be obtained and their energy depends on details such as its total angular and spin momentum (multiplet structure) [21]. For the 3p lines we see within the limits of statistical accuracy no dependence of the line shape on momentum. Also, the momentum distribution follows a typical p-type behaviour (a sharp minimum in intensity at zero momentum). The momentum measured in an EMS experiment on correlated systems is the recoil momentum, i.e. the total change in momentum of the target. If, as a consequence of the ionization, a valence electron is localized, one would expect the total momentum transferred to the target to be different from that of the ejected core electron by itself. If the excess width is due to an unresolved multiplet structure then final states with different angular momenta could have different recoil momentum distributions and thus the shape of the core level could depend on the momentum. No theoretical models describing these cases have been developed so far.

More promising were the results from a separate measurement of the V 2p and O 1s core levels. These results are shown in figure 6. These spectra were obtained by raising the gun

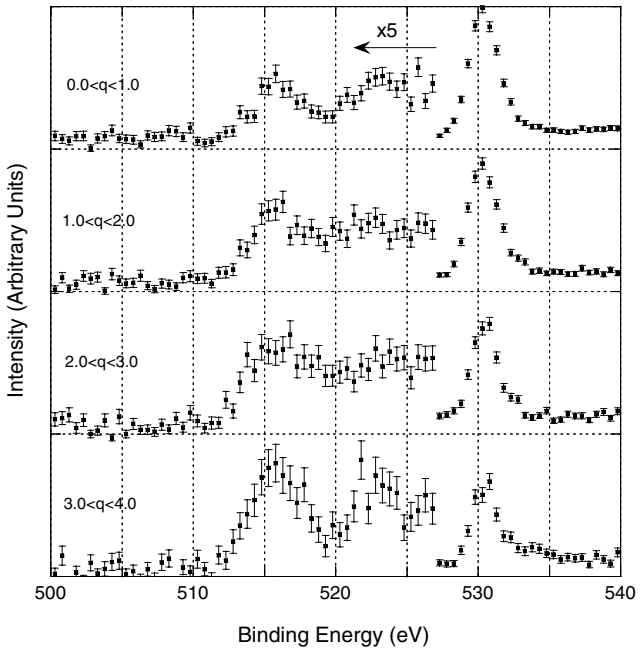

Figure 6. The spectra obtained for the O 1s and V 2p core levels as a function of momentum. The oxygen peak is observed near 530 eV; it has a decreasing amplitude with increasing momentum. The V 2p doublet, near 515 and 523 eV, is plotted on a 5× expanded scale, its intensity increases with momentum and its shape appears momentum dependent.

voltage by 500 eV. These relative deep core levels are very broad in momentum space, and hence their density is low, resulting in low count rates. These spectra were obtained in a measurement lasting 7 days. Using hydrogenic wavefunctions we estimate that the density of the O 1s wavefunction decreases from its maximum at zero momentum to 50% at 3 au, whereas the V 2p intensity increases from zero at 0 au to a maximum near 4 au. Indeed, in the experiment the intensity of the O 1s feature slowly decreases with momentum, whereas the intensity of the V 2p line increases. More interestingly, there seems to be a change in shape of the 2p lines with momentum. In the spectrum at low momentum (0–1 au range) and in the spectrum for the highest accessible momentum range (3–4 au) the doublet is well resolved, whereas in the intermediate momentum range it is not. This could be attributed to different momentum distributions of the large number of unresolved final states contributing to the observed spectra (see e.g. [21]). However no theory exist for EMS of such core levels.

In figure 7 we show more spectra of V metal at selected momentum intervals, as well as momentum distributions at several binding energy intervals. These experimental results are compared with an LMTO calculation convoluted with 1 eV energy resolution. This theory underestimates the width of the observed peaks, especially those at larger binding energies. This is mainly due to lifetime broadening. In spite of this it appears that the calculated value of the total band width of 6.57 eV is in good agreement with the experimentally observed value of 6.5 ± 0.4 eV. This is in contrast to copper where the observed total valence band width as measured by EMS or photoemission exceeds the width predicted by the FP-LMTO theory by about 0.6 eV [5]. Unfortunately, the few angular-resolved photoemission studies published for vanadium metal do not allow for the determination of the total occupied band width, as the photoemission spectra are dominated by emission from the 3d electrons [22].

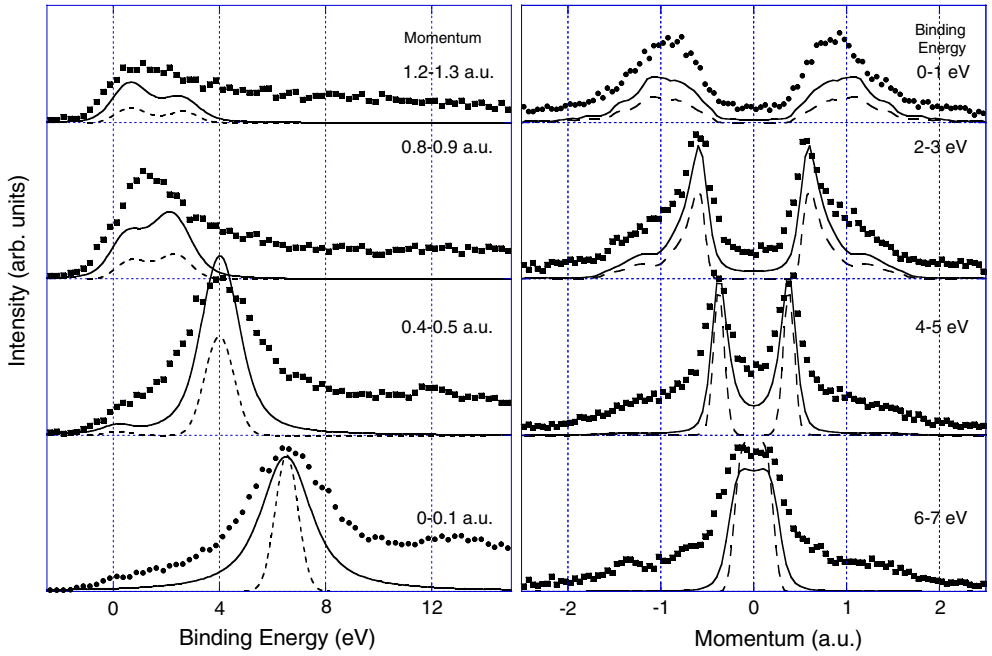

Figure 7. Spectra of V metal for selected momentum intervals (left panel) and momentum densities for selected binding energy intervals (right panel) for a V metal film. The dashed line is obtained from the LMTO theory (broadened by 1 eV to mimic the experimental resolution) integrated over the same range as the experimental spectra. The full line is obtained in the same way, but now semi-empirical lifetime broadening has been added to the calculations.

Also shown in figure 7 are the results of the FP-LMTO theory convoluted with a lifetime broadening based on free electron gas calculations [10]. This improves the overall agreement between theory and experiment considerably, but the experimental width at larger binding energy is still larger than the calculated one, suggesting that the theoretical approach underestimates the lifetime broadening. The main discrepancy is now a smooth background due to inelastic multiple scattering and intrinsic satellites. No attempt has been made yet to disentangle both contributions, a problem that is complicated due to the presence of an interface component in the sample. Generally, the intensity near the Fermi level (mainly d electrons) and at larger binding energy are described reasonably well by the theory.

Now let us have a closer look at the valence band of V_2O_3. The spectra for selected momentum intervals are plotted in figure 8. The position and width of the O 2p and O 2s feature are in reasonable agreement with those observed by XPS [23]. The observed structures are considerably wider than our energy resolution. This applies to the measurement of the polycrystalline sample as well as the single-crystal measurement. Thus the excess width is not caused by directional averaging in the polycrystalline case. This is not too surprising as the calculated anisotropy in dispersion, as shown in figure 2, is not very large. In order to facilitate a comparison between theory and experiment we have convoluted the calculated spectra with an energy resolution of 3 eV and plotted these calculations in the same graph. There are two obvious discrepancies between the calculated and measured distributions.

In the first place, the separation between the O 2s and O 2p parts of the valence band is larger in the experiment than predicted by the FP-LMTO method by about 2 eV. This discrepancy is not unique for V_2O_3, and is observed for most oxides studied by EMS [24–27].

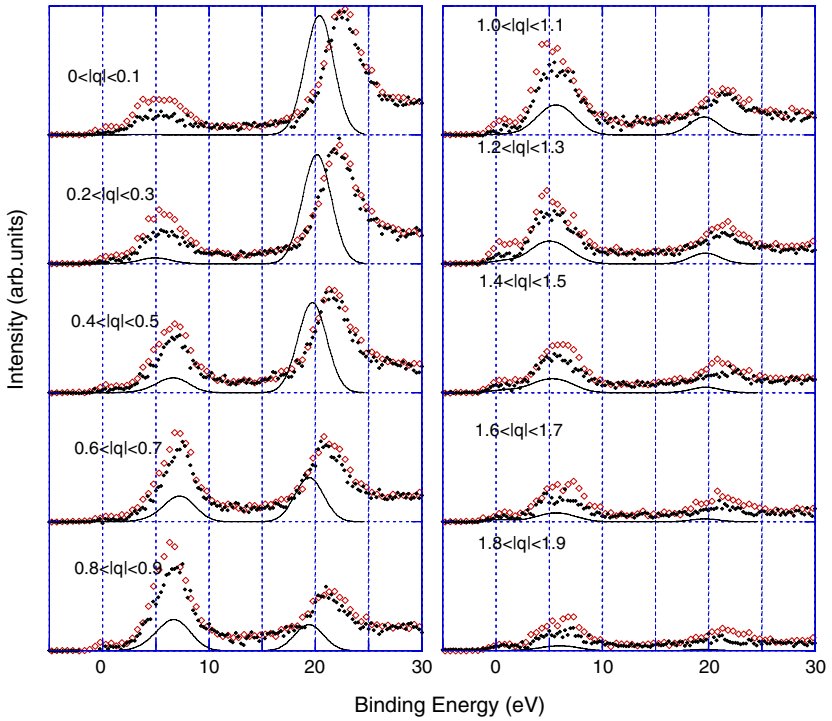

Figure 8. Spectra of V_2O_3 for the valence band region for momentum intervals as indicated (dots, polycrystalline film; diamonds, single-crystal film along Γ–K direction) and the calculated spectra for the polycrystalline case, based on the LMTO theory, but broadened by 3 eV (full line).

It could be a problem related to density functional theory (DFT). Bandgaps in semiconductors are always underestimated in DFT calculations [28]. The underestimation of the gap between the inner and outer valence bands of the oxides may have the same roots. A *GW* calculation (based on the Green function *G* calculated using the screened Coulomb interaction *W* [29]) of these oxides would be desirable. Indeed, for the ionic compound LiF Shirley *et al* [30] found that quasiparticle calculations within the *GW* scheme gave a 1.7 eV larger separation of the F 2s and 2p bands than a band structure calculation within the DFT scheme. The observed discrepancies for V_2O_3 and other oxides are thus in line with the calculated self-energy effects for LiF.

A second discrepancy, that is also observed for all other oxides studied by EMS so far [24–27], is that the ratio between the observed intensity of the O 2p derived band relative to that of the O 2s derived band differs from the calculated one by at least a factor of two. This is obvious in figure 8. The maximum intensity of the 2s level is at zero momentum. In the experiment the maximum 2p intensity is near 0.8 au. The observed 2p intensity near 0.8 au is nearly the same as the 2s intensity at 0 au. However, the theory predicts that the maximum 2s intensity exceeds the maximum 2p intensity by about a factor of three.

From gas-phase measurements we know that, for example, in the case of argon a considerable amount of intensity associated with the inner valence 3s electrons appears in the form of satellites at higher binding energy [31]. Only 5% of the Ar 3p intensity appears in the form of satellites, whereas 45% of the 3s intensity appears as satellites. Considering the oxygen ions as a closed shell system, we could expect similar values here. Unfortunately, we

cannot distinguish between the background due to inelastic multiple scattering (energy loss of the incoming or outgoing keV electrons) and that due to satellites. Moreover, for the case of neon, which resembles the oxygen ions much more closely, the gas-phase measurements show a satellite intensity for the 2p level of 8% and for the 2s level 15% [32]. This would change the intensity ratio only marginally. Hence this is not likely to explain the observed 2s/2p intensity ratio.

The single-crystal film shows even more intensity in the 2p part of the spectrum than in the polycrystalline film. This applies as well to the zero-momentum spectrum, where, without multiple scattering, no 2p intensity is expected at all. Due to diffraction, elastic scattering effects can be rather different for the single-crystal film. Assuming that a similar elastic multiple-scattering contribution exists for spectra at other momentum values, then one should subtract this contribution before comparing with theory. Indeed, the remaining intensity is in much better agreement with the theory.

For a fair comparison of the 2s/2p intensity ratio the 2s intensity should be corrected for multiple scattering as well. However, the 2s intensity is less affected by these effects. This level is occupied in momentum space only in a small region near the origin. Hence only elastic scattering events with a small range of momentum transfers can increase the 2s intensity at a certain momentum. For the more diffuse 2p level (accommodating three times as many electrons) elastic scattering over a much larger momentum range can contribute to the intensity in a spectrum taken at a certain momentum. Monte Carlo simulations show this tendency, but not as strongly as the experiment.

To see if the momentum dependence of the intensity of the levels can shed any light on the problem, we fitted the peaks in the binding energy spectra with a Gaussian on a linear background. The area of the Gaussians is plotted in figure 9 as a function of momentum. The solid lines represent the calculated momentum densities for the FP-LMTO model of V_2O_3 and the dashed lines correspond to atomic O and V orbital densities. The theory has been normalized to the experiment separately for the O 2p, O 2s and V 3d levels. The measured shapes compare well. The 2p level shows, as expected, a sharp minimum at zero momentum as this corresponds to a node in the wavefunction. Such deep minima are only observed after careful alignment of the scattering geometry [33]. The residual intensity at zero momentum is in line with expectations and is due to finite momentum resolution and low levels of elastic multiple scattering present even at the high electron energies deployed here. The intensity distribution integrated over the total 2s and, to a lesser degree, the 2p part resembles the atomic 2s and 2p levels for both the experiment and the FP-LMTO calculation. The total O 2p intensity distribution is, relative to the atomic O 2p intensity distribution, slightly shifted to higher momentum values. This could be interpreted as a consequence of some hybridization of the O 2p level with V 3d levels, as can be inferred from band structure calculations [13]. In contrast, for the case of SiO_2, where 3d electrons play no significant role, the calculated and measured outer valence band momentum density profile resembles that of the atomic O 2p profile more closely than in the present V_2O_3 case [26].

We also plot in figure 9 the intensity distribution of the shoulder near the Fermi level. The shoulder is due to the V 3d derived bands. It is a weak signal on a broad background. However the experiment and theory both show a relatively sharp feature at 1.2 au. It is much sharper than the atomic V 3d distribution. The fact that the FP-LMTO theory predicts it correctly means that the electrons are coherent i.e. can be described by Bloch functions.

In spite of the polycrystalline nature the dispersion in the outer valence band is clearly resolved. To demonstrate this, we plot in figure 10 only the outer valence band together with the theory convoluted by only 1 eV energy resolution. The theory predicts that more than one component should be visible near 1 au of momentum. The main intensity in this plot, due to

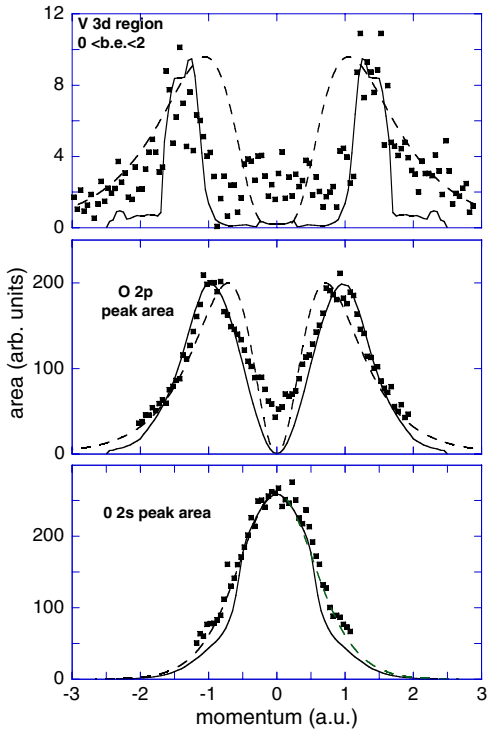

Figure 9. The measured intensity for the O 2s, O 2p and V 3d part of the spectrum, compared with the calculated density. The solid line is the momentum density obtained by integrating the FP-LMTO results over binding energies corresponding to the O 2s, O 2p and V 3d parts of the SMD. The dashed lines are the *atomic* O 2s, O 2p and V 3d momentum densities.

the O 2p part of the valence band, follows the shape of the theory nicely, but is generally not as sharp as one would expect based on a 1 eV energy resolution. Lifetime broadening is expected to be minor here, as there are no orbitals at lower binding energy with a large density at the oxygen ions.

Between 1.2 and 1.5 au of momentum there is a shoulder visible in the experiment, just below the Fermi level. The theory has a separate peak with similar intensity. It is this shoulder that causes the peaks in the V 3d momentum distribution, as plotted in the top panel of figure 9.

For the single-crystal film we measured the spectra momentum density along the Γ–M direction and the Γ–K direction. For the O 2p and O 2s derived bands no major differences were found in dispersion or intensity along both directions. The peak width was still larger than the experimental resolution. The origin of this broadening is not understood. Hence the splitting of the O 2p part of the spectrum, predicted for the Γ–M (see figure 2) direction, is not observed. The calculated differences in dispersion along both directions are smaller than the *observed* peak width.

5. Conclusions and outlook

We report on the initial EMS experiments on vanadium and one of its oxides. Even the spectra obtained from samples prepared by simple evaporation on a thin carbon film are a rich source of information on the electronic structure of these materials. We also succeeded in growing

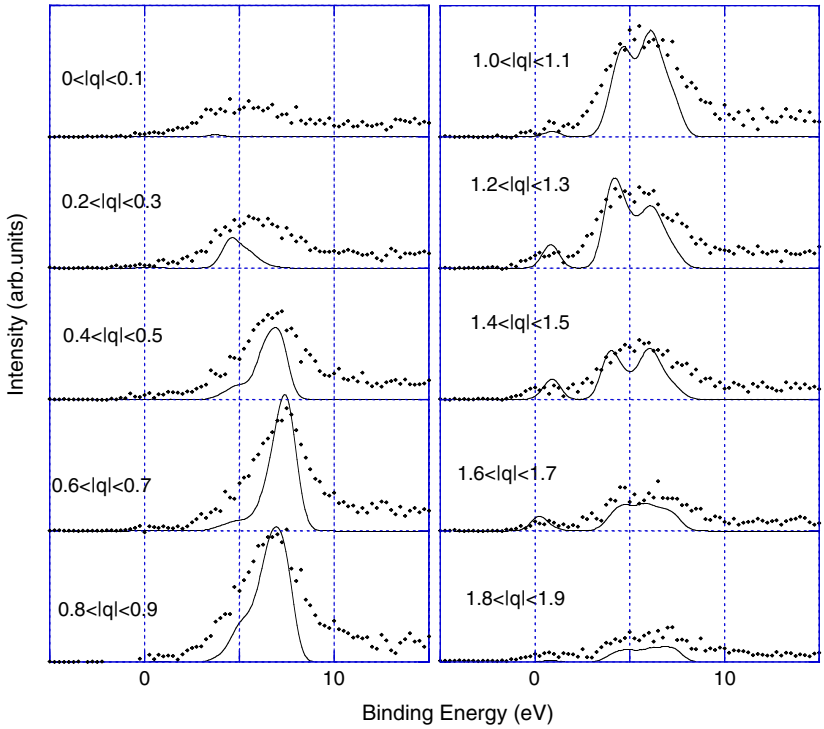

Figure 10. The measured outermost valence band region for polycrystalline V_2O_3, for momentum intervals as indicated (dots) together with the spherically averaged theory (full line).

single-crystal films of V_2O_3. The calculated anisotropy of the dispersion was small and could not be confirmed by the experiment. This is in contrast to single-crystal films of silicon [3, 4] and copper [5], where the experimental single-crystal results clearly resolve the anisotropy of the electronic structure.

These measurements of a metallic phase of vanadium oxide open the way for studying an insulating phase, which cannot be described by band structure theory. Rather than changing the temperature the insulating phase can be accessed by co-evaporation of small amounts of chromium together with vanadium in an oxygen atmosphere, forming a Mott–Hubbard insulator. The momentum distributions observed under these conditions at small binding energies are expected to be different from those observed for pure V_2O_3.

Replacing a few per cent of vanadium by chromium in V_2O_3 causes a change from a metal to an insulator (see e.g. [34, 35]). This phase transition is often considered to be a prime example of the transition from a metal to a Mott–Hubbard insulator. The current sharp peak in the momentum distribution near E_f for the metal phase is a consequence of the Bloch nature of these electrons (band structure effects). If the V 3d electrons would be localized on a single V atom, as would be the case in an Mott–Hubbard insulator, one would expect a broad distribution in momentum space. This is a direct consequence of the Heisenberg uncertainty principle as localization in real space should correspond to a broad distribution in momentum space. In the insulating phase, not predicted by band structure calculations, the electrons are considered localized (incoherent), and intuitively one would expect a momentum distribution to be more like that of an isolated atom (much broader). Thus, these plausible experiments could provide a new window on the Mott–Hubbard phase transition.

The fact that the *total* 2s and 2p intensity resembles the modulus square of the atomic 2s and 2p wavefunction does not mean that these levels are localized. If we take slices over a narrow energy window we would see a much sharper distributions in momentum space, as can be inferred from figure 4. These distributions are somewhat broadened due to energy resolution of the experiment and lifetime broadening.

Thus in the present case the 3d level is sharp in momentum space, because the band is not full, and only those k-values are occupied that correspond to the lowest energy states. In the Mott–Hubbard insulating phase it should be as broad as the *atomic* V 3d momentum distribution. The momentum distributions of the 2s and 2p parts of the spectrum should not be influenced by the phase transition.

The broad V 3p and V 2p peaks in V_2O_3 are another challenge. Should they have the same momentum distribution as the atomic 3p peak, or, assuming the extra width is due to interactions with the V 3d electrons, do they have a different dependence of intensity on momentum dependence, or will their shape depend on energy? The 2p spectra seem to indicate that the line shape is momentum dependent. Theories describing these phenomena would certainly stimulate further experimental endeavours.

Acknowledgments

This research was possible due to a grant of the Australian Research Council. The authors want to thank Erich Weigold for carefully reading the manuscript.

References

[1] Weigold E and McCarthy I E 1999 *Electron Momentum Spectroscopy* (New York: Kluwer–Academic Plenum)
[2] Vos M, Kheifets A S, Sashin V and Weigold E 2003 *AIP Conf. Proc.* **652** 491
[3] Vos M, Bowles C, Kheifets A S, Sashin V A, Weigold E and Aryasetiawan F 2004 *J. Electron Spectrosc. Relat. Phenom.* **137–140** 629
[4] Bowles C, Kheifets A, Sashin V, Vos M and Weigold E 2004 *J. Electron Spectrosc. Relat. Phenom.* **141** 95
[5] Vos M, Kheifets A, Bowles C, Chen C, Weigold E and Aryasetiawan F 2004 *Phys. Rev.* B **70** 20511
[6] Vos M, Cornish G P and Weigold E 2000 *Rev. Sci. Instrum.* **71** 3831
[7] Vos M and Bottema M 1996 *Phys. Rev.* B **54** 5946
[8] Dupuis A C, Haija M A, Richter B, Kuhlenbeck H and Freund H J 2003 *Surf. Sci.* **539** 99
[9] Kheifets A S, Lun D R and Savrasov S Y 1999 *J. Phys.: Condens. Matter* **11** 6779
[10] Lundqvist B 1968 *Phys. Kondens. Mater.* **6** 193
[11] Wyckoff R 1963 *Crystal Structures* (New York: Interscience)
[12] Slater J C 1965 *Quantum Theory of Molecules and Solids* (New York: McGraw-Hill)
[13] Mattheis L 1994 *J. Phys.: Condens. Matter* **6** 6477
[14] Lábár J 2000 *Eurem* **12** 1379
[15] Surnev S, Ramsey M G and Netzer F P 2003 *Prog. Surf. Sci.* **73** 117
[16] Vos M and McCarthy I E 1997 *Am. J. Phys.* **65** 544
[17] Vos M, Kheifets A S, Sashin V A, Weigold E, Usuda M and Aryasetiawan F 2002 *Phys. Rev.* B **66** 155414
[18] Powell C J 1995 *Appl. Surf. Sci.* **89** 141
[19] Vos M, Kheifets A S, Weigold E and Aryasetiawan F 2001 *Phys. Rev.* B **63** 033108
[20] Sawatzky G and Post D 1979 *Phys. Rev.* B **20** 1546
[21] Taguchi M *et al* 2005 *Phys. Rev.* B **71** 155102
[22] Perić B, Valla T, Milun M and Pervan P 1995 *Vacuum* **46** 1181
[23] Zimmermann R, Claessen R, Reinert F, Steiner P and Hüfner S 1998 *J. Phys.: Condens. Matter* **10** 5697
[24] Bolorizadeh M, Sashin V, Kheifets A and Ford M 2004 *J. Electron Spectrosc. Relat. Phenom.* **141** 27
[25] Soulé de Bas B, Dorsett H E and Ford M J 2003 *J. Phys. Chem. Solids* **64** 495
[26] Fang Z *et al* 1998 *Phys. Rev.* B **57** 4349
[27] Sashin V A, Bolorizadeh M A, Kheifets A S and Ford M J 2003 *J. Phys.: Condens. Matter* **15** 3567
[28] Kotani T and van Schilfgaarde M 2002 *Solid State Commun.* **121** 461

[29] Hedin L and Lundqvist S 1969 *Solid State Phys.* **23** 1
[30] Shirley E, Terminello L J, Klepeis J E and Himpsel F J 1996 *Phys. Rev.* B **53** 10296
[31] McCarthy I E, Pascual R, Storer P and Weigold E 1989 *Phys. Rev.* A **40** 3041
[32] Samardzic O, Braidwood S W, Weigold E and Brunger M J 1993 *Phys. Rev.* A **48** 4390
[33] Vos M, Sashin V, Bowles C, Kheifets A and Weigold E 2004 *J. Phys. Chem. Solids* **65** 2035
[34] McWhan D and Remeika J 1970 *Phys. Rev.* B **2** 3734
[35] Mo S-K *et al* 2004 *Phys. Rev. Lett.* **93** 076404